ACS OMEGA

http://pubs.acs.org/journal/acsodf

Article

Design, Synthesis, and Biological Evaluation of the First Radiometalated Neurotensin Analogue Targeting Neurotensin Receptor 2

Sacha Bodin, Santo Previti, Emmanuelle Jestin, Delphine Vimont, Imade Ait-Arsa, Frédéric Lamare, Emmanuelle Rémond, Elif Hindié, Florine Cavelier,*,# and Clément Morgat*,#

Cite This: *ACS Omega* 2023, 8, 6994−7004

Read Online

ACCESS | Metrics & More | Article Recommendations | Supporting Information

ABSTRACT: Neurotensin receptor 2 (NTS_2) is a well-known mediator of central opioid-independent analgesia. Seminal studies have highlighted NTS_2 overexpression in a variety of tumors including prostate cancer, pancreas adenocarcinoma, and breast cancer. Herein, we describe the first radiometalated neurotensin analogue targeting NTS_2. JMV 7488 (DOTA-$(\beta Ala)_2$-Lys-Lys-Pro-(D)Trp-Ile-TMSAla-OH) was prepared using solid-phase peptide synthesis, then purified, radiolabeled with ^{68}Ga and ^{111}In, and investigated *in vitro* on HT-29 cells and MCF-7 cells, respectively, and *in vivo* on HT-29 xenografts. [^{68}Ga]Ga-JMV 7488 and [^{111}In]In-JMV 7488 were quite hydrophilic ($logD_{7.4} = -3.1 \pm 0.2$ and -2.7 ± 0.2, respectively, $p < 0.0001$). Saturation binding studies showed good affinity toward NTS_2 ($K_D = 38 \pm 17$ nM for [^{68}Ga]Ga-JMV 7488 on HT-29 and 36 ± 10 nM on MCF-7 cells; $K_D = 36 \pm 4$ nM for [^{111}In]In-JMV 7488 on HT-29 and 46 ± 1 nM on MCF-7 cells) and good selectivity (no NTS_1 binding up to 500 nM). On cell-based evaluation, [^{68}Ga]Ga-JMV 7488 and [^{111}In]In-JMV 7488 showed high and fast NTS_2-mediated internalization of 24 ± 5 and $25 \pm 11\%$ at 1 h for [^{111}In]In-JMV 7488, respectively, along with low NTS_2-membrane binding (<8%). Efflux was as high as $66 \pm 9\%$ at 45 min for [^{68}Ga]Ga-JMV 7488 on HT-29 and increased for [^{111}In]In-JMV 7488 up to $73 \pm 16\%$ on HT-29 and $78 \pm 9\%$ on MCF-7 cells at 2 h. Maximum intracellular calcium mobilization of JMV 7488 was $91 \pm 11\%$ to that of levocabastine, a known NTS_2 agonist on HT-29 cells demonstrating the agonist behavior of JMV 7488. In nude mice bearing HT-29 xenograft, [^{68}Ga]Ga-JMV 7488 showed a moderate but promising significant tumor uptake in biodistribution studies that competes well with other nonmetalated radiotracers targeting NTS_2. Significant uptake was also depicted in lungs. Interestingly, mice prostate also demonstrated [^{68}Ga]Ga-JMV 7488 uptake although the mechanism was not NTS_2-mediated.

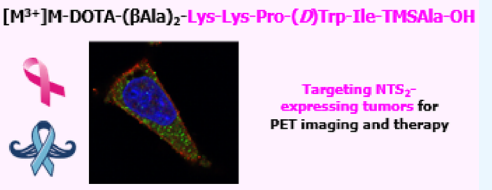

INTRODUCTION

G-protein coupled receptors (GPCRs) represent numerous targets for drug development,[1] particularly in nuclear medicine. Recent advances in nuclear oncology include the use of [^{68}Ga]Ga-DOTATOC and [^{177}Lu]Lu-DOTATATE for diagnosis and peptide receptor radionuclide therapy (PRRT) of digestive neuroendocrine tumors overexpressing the somatostatin receptor subtype 2 (SST_2), which is part of the class A GPCR family. Among this same family, neurotensin (NT) receptors represent also promising targets for imaging and therapy. Neurotensin is a 13 amino acid neuropeptide,[2] which binds to three receptors, two GPCRs, namely, NTS_1 and NTS_2, and the single transmembrane domain NTS_3/sortilin receptor. NTS_1 and NTS_2 are widely expressed in the central nervous system (CNS) where they are involved in opioid independent analgesia, hypothermia, and psychiatric effects,[3] but they also exhibit peripheral actions.[4,5]

Numerous NTS_1 targeting ligands carrying the pharmacophore NT(8-13) hexapeptide sequence (H-Arg-Arg-Pro-Tyr-Ile-Leu-OH)[6,7] have been developed and studied in different types of peripheral tumors, such as colorectal cancer, prostate adenocarcinoma, breast cancer, or pancreatic cancer.[8−12] Contrarily, NTS_2 targeting peptides have been studied for their central opioid-independent analgesic potency.[13−17] Whereas very few analogues have been developed for imaging of peripheral tumors,[18] NTS_2's role in tumor development remains unclear and requires more investigations. Indeed, in prostate cancer, NTS_2 mRNA expression was found only in malignant well-differentiated (androgen receptors +) cell-lines.[19] A recent study also demonstrated its involvement in apoptosis resistance in B-cell chronic lymphocytic leukemia.[20]

Only few studies have investigated the expression of NTS_2 in normal organs. In healthy tissues, NTS_2 has been found to be expressed in lungs.[21]

Herein, we report the pharmacological and biological properties of JMV 7488, a new silylated NTS_2-targeting hexapeptide radiolabeled with gallium-68 and indium-111. This ligand is derived from the *N*-terminal elongation of JMV

Received: December 7, 2022
Accepted: January 30, 2023
Published: February 10, 2023

5504, a modified NT(8-13) analogue, which has high affinity and selectivity toward the NTS_2 receptor.[22]

MATERIALS AND METHODS

Chemistry, radiolabeling procedure, determination of the octanol/water partition coefficient, cell culture, western blot, confocal imaging, and *blood plasma* stability methods are fully presented in the Supporting Information.

***In Vitro* Studies.** HT-29 and MCF-7 cells were seeded into 24-wells plates at the density of 2×10^5 cells per well, the day before the experiment. The plates were incubated at 37 °C and 5% CO_2. All the binding and internalization experiments were carried out in quadruplicate and efflux studies in octuplicate.

Saturation Binding Studies. Plates were stored at 4 °C for 30 min in order to reduce cell processing and then incubated for 2 h at 37 °C with 250 μL of complete medium containing the radiolabeled peptide at increasing concentrations (0.1, 1, 10, 100, 250, and 500 nM) with and without saturation ligands (neurotensin, a specific agonist of NTS_1 or levocabastine, a specific agonist of NTS_2, final concentration of 1 μM). After incubation, cells were rinsed twice with ice cold DPBS (250 μL, 14190-144, Gibco). Then, cells were lysed with NaOH 1 M (750 μL) to collect the bound fraction. Radioactivity of each fraction was determined in a gamma-counter (Wizard2, PerkinElmer, USA). Affinity (K_D) was determined by nonlinear regression using Prism 6.01 software (GraphPad Software Inc., USA). Experiments were performed three times in quadruplicates.

Cell-Associated Radioactivity and Internalization Studies. A total of 1 MBq of [^{68}Ga]Ga-JMV 7488 or 50 kBq of [^{111}In]In-JMV 7488 in 250 μL of complete medium with and without 1 μM of saturation ligands was added in each well. Plates were incubated for 10, 30, or 60 min (plus 120 and 240 min for ^{111}In radiolabeled JMV 7488) at 37 °C. Three minutes before the selected time point, plates were stored at 4 °C to stop the internalization process. Media were removed, and wells were rinsed three times with ice cold DPBS (250 μL). A total of 250 μL of sodium acetate (20 mM, pH 5) was added in each well twice and then collected in tubes after 5 min incubation. Then, cells were lysed with NaOH 1 M (750 μL) to collect the bound fraction. Radioactivity of each fraction was determined in a gamma-counter. Cell-associated radioactivity results are expressed as percentage of specific binding. Experiments were performed four times in quadruplicates.

Efflux Studies. A total of 1 MBq of [^{68}Ga]Ga-JMV 7488 or 50 kBq [^{111}In]In-JMV 7488 in 250 μL of complete medium was added in each well. Plates were incubated 30 min at 37 °C. Media were removed, and cells were rinsed with ice cold DPBS (250 μL). A total of 250 μL of sodium acetate (20 mM, pH 5) was added in each well and removed after 5 min of incubation. Cells were rinsed again with ice cold DPBS (250 μL). Then, 250 μL of medium were added in each well and plates were incubated for 5, 15, 30, or 45 min (or 5, 15, 60, and 120 min for ^{111}In radiolabeled JMV 7488) at 37 °C. Media were collected in tubes, and each well was rinsed twice with ice cold DPBS (250 μL). Then, cells were lysed with NaOH 1 M (750 μL) to collect the bound fraction. Radioactivity of each fraction was determined in a gamma-counter. Results are expressed as percentage of total binding. Experiments were performed three times in octuplicate.

Calcium Imaging Assay. HT-29 cells were cultured as previously described. The day before the experimentation, cells were grown on 15 mm Thermanox glass slides (Thermofischer, USA) in 12-wells plates at the density of 5×10^5 cells in 500 μL of complete culture medium. Night incubation at 37 °C and 5% CO_2 allows cell adherence on the slides. Glass slides were individually loaded for 30 min in the dark with a 500 μL loading solution containing 100 μM fluo-8 AM (ATT Bioquest, USA), 0.4% (w/v) pluronic acid (AAT Bioquest, USA), and 2.5 mM probenecid (Invitrogen, Thermofischer, USA) into RPMI medium. Slides were then placed in a recording chamber perfused with buffer solution (containing (in mM): 130 NaCl, 3 KCl, 2.5 $CaCl_2$, 1.3 $MgSO_4$, 0.58 NaH_2PO_4, 25 $NaHCO_3$, and 10 glucose) equilibrated with 95% O_2/5% CO_2, adjusted to pH 7.4 at room temperature. A 10 min delay was respected to wash out extracellular fluo-8 AM and enable fluo-8AM intracellular hydrolysis. Increasing concentrations (10^{-11} to 10^{-5} M) of JMV 7488 were added *via* a rapid perfusion system. Positive control experiments were performed by adding similar concentrations of levocabastine. Imaging of intracellular Ca^{2+} changes was performed following excitation of cells at 490 nm with analysis of fluorescence emission at 514 nm using an Eclipse E600FN microscope (Nikon, Japan) coupled with an Infinity 3 detector (Lumenera, Canada). Changes in fluorescence (F_T) were calculated for each cell relative to the averaged baseline fluorescence before stimulation (F_{REST}) and expressed as $\Delta F/F$ (%) = $[(F_T - F_{REST})/(F_{REST})] \times 100$. The calcium mobilization assay was performed twice in duplicate, and 20 cells were manually analyzed.

***In Vivo* Studies.** Animal experiments have been approved and permitted by the Ethics committee n°114 (reference APAFIS#26960-2020061008304944 v4) and were conducted according to European and national guidelines. All the animals were maintained at a constant temperature (24 ± 1 °C) and a hygrometry between 55 and 65% under a 12 h light/dark cycle and permitted free access to food and water.

HT-29 Xenograft Model. Eight weeks old female Balb-c nude mice have been purchased from JANVIER LABS, and quarantined for 2 weeks. Animals are fed ad libitum and maintained in a HEPA-filtered environment with cages, food, and bedding sterilized by autoclaving.

Under anesthesia with isoflurane (2% in air mixture), Balb-c nude mice were injected subcutaneously in the right flank with 1×10^6 HT-29 cells suspended in 100 μL of 50:50 Matrigel/collagen I. Tumor growth was monitored externally using calipers. Biodistribution and PET/CT imaging studies were performed in mice when tumor volume reached approximatively 150 mm^3.

Micro-PET/CT Imaging. The preclinical imaging studies were performed on a multimodality imaging system (Triumph II, PET/SPECT/CT, Trifoil Imaging, Chatsworth, USA). Mice were anesthetized with isoflurane (3%) and placed under the PET modality on a temperature-controlled bed. Injections of the radiotracers were proceeded in the caudal lateral vein using an insulin syringe 29-gauge under the camera to get the bolus. Four mice were injected with [^{68}Ga]Ga-JMV 7488 (6.58 ± 1.54 MBq, 4.3 ± 3.6 nmol, ~50 μL diluted in 150 μL of saline before administration), and four mice were injected with 0.5 μmol levocabastine 15 min prior to radiotracer injection (6.16 ± 1.21 MBq). PET acquisitions were done under anesthesia (isoflurane 3% induction and 1.5% maintenance in air) during 75 min. CT acquisitions were carried out at the end of the experiment. Animals were then sacrificed 90 min post-injection, and the organs were collected as described below.

https://doi.org/10.1021/acsomega.2c07814
ACS Omega 2023, 8, 6994−7004

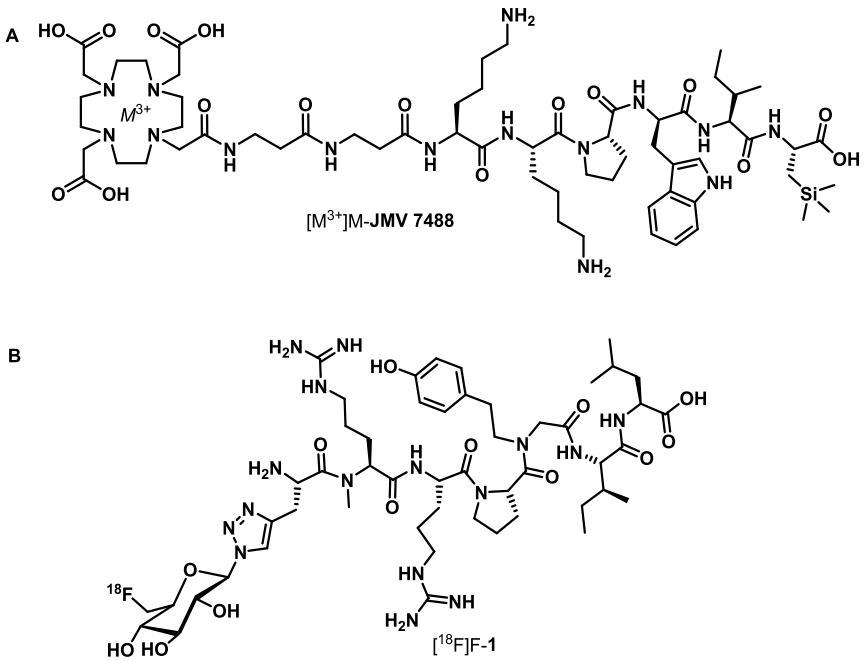

Figure 1. (A) Structure of [M^{3+}]M-JMV 7488 developed in this study. M^{3+} stands for ^{68}Ga or ^{111}In in this study. Coordination bonds are not figured out. (B) Structure of the ^{18}F-labeled neurotensin peptoid [^{18}F]F-1 previously developed in the literature to target the neurotensine receptor 2.

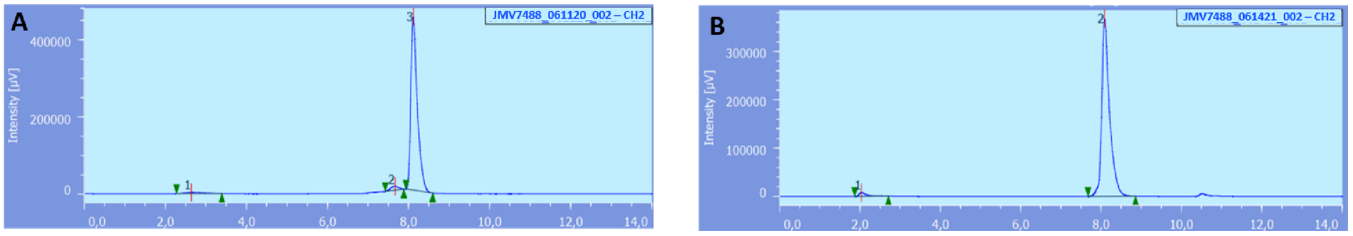

Figure 2. Radio-HPLC chromatogram of [^{68}Ga]Ga-JMV 7488 (A) and [^{111}In]In-JMV 7488 (B).

PET data were reconstructed using the OSEM 3D method. CT files were reconstructed using a Feldkamp algorithm after obtaining an isotropic voxel size of 0.170 mm.

Biodistribution Studies. Four mice were injected with [^{68}Ga]Ga-JMV 7488 (6.58 ± 1.54 MBq, 4.3 ± 3.6 nmol, ~50 μL diluted in 150 μL of saline before administration), and four mice were injected with 0.5 μmol levocabastine 15 min prior to radiotracer injection (6.16 ± 1.21 MBq). Solutions were injected into the tail vein. Animals were sacrificed 90 min post-injection by an intracardiac puncture. Blood, heart, lungs, liver, kidneys, spleen, stomach, intestines, muscle, bone, prostate, brain, and HT-29 tumor were collected. Organs were weighed and γ-counted (Wizard 2470, Perkin Elmer). Uptake levels were expressed as percentage of injected dose per gram of tissue (%ID/g).

Statistical Analyses. Statistical analyses were performed using Prism v6.01 software (GraphPad Software Inc., USA). Unpaired data were used. Quantitative values were expressed as means ± SD. Statistical analysis with at least three groups were performed with the multiple *t*-tests corrected for multiple comparisons using the Holm Sidak method. Comparisons between two groups were performed using the bilateral nonparametric Mann−Whitney test. A *P*-value of <0.05 was considered significant.

Purity Statement. All compounds are >95% pure by HPLC and LCMS analysis. Representative traces are provided in the Supporting Information.

RESULTS

Chemistry. The unnatural amino acid trimethylsilylalanine (TMSAla) carrying the fluorenylmethyloxycarbonyl (Fmoc) as the protecting group was synthesized following the synthetic pathway we already reported.[23] After that, the obtained Fmoc-TMSAla-OH was loaded on 2-chlorotrityl chloride (2-CTC) resin,[24] which was previously treated with $SOCl_2$ to optimize the reactive sites. A loading of 0.8 mmol/g was detected with UV spectroscopy. On the contrary, the loading of Fmoc-TMSAla-OH resulted to be unproductive if untreated resin was used. The desired NT analogue JMV 7488 (Figure 1) was synthesized using the solid phase peptide synthesis (SPPS) approach with a yield of 31% (0.1 mmol scale). Even though the yield is moderately low, LC−MS analysis of the crude product after final cleavage showed a major peak with minimum amounts of by-products. This good HPLC profile allowed us to purify the desired product very easily. All data concerning the synthesis and characterization of JMV 7488 are detailed in the Supporting Information.

^{68}Ga and ^{111}In Radiolabeling. Radiolabeling were achieved with moderate yields of 53.88 ± 8.34 (^{68}Ga, decay-

https://doi.org/10.1021/acsomega.2c07814
ACS Omega 2023, 8, 6994−7004

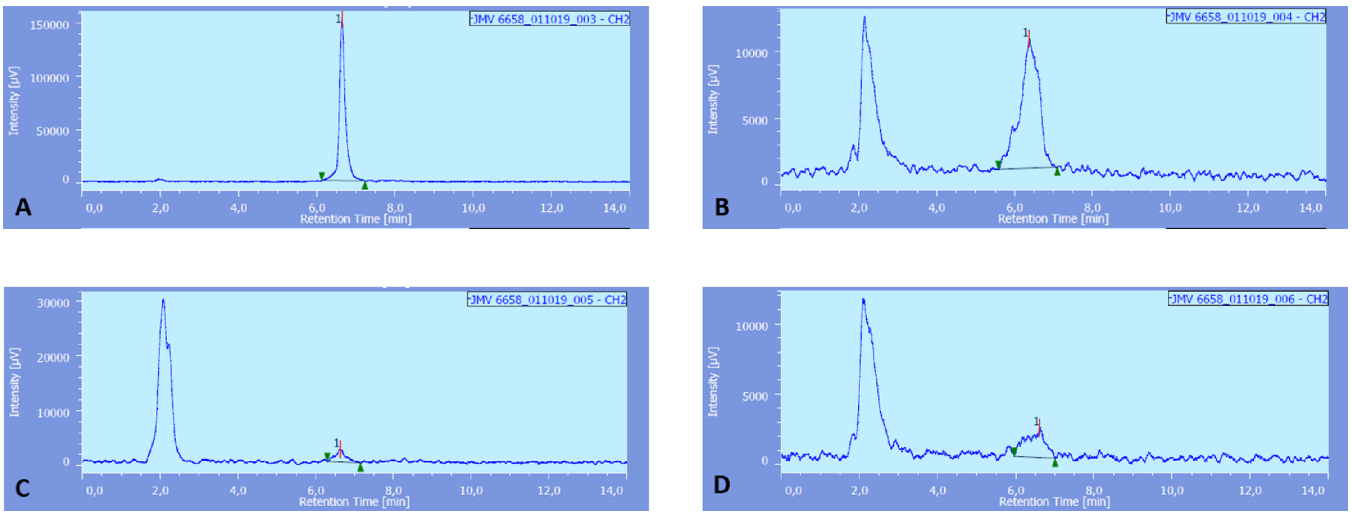

Figure 3. Radio-HPLC chromatograms of [^{68}Ga]Ga-JMV 7488 in human plasma 0 (A), 15 (B), 30 (C), and 45 min (D) after incubation.

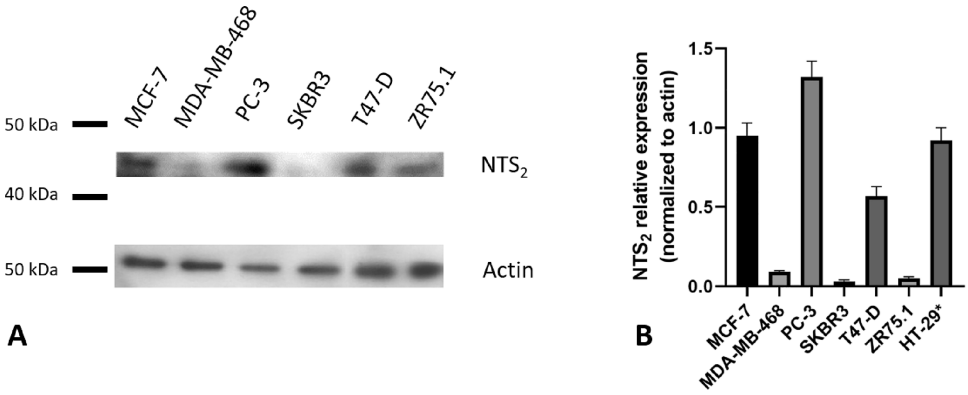

Figure 4. (A) Representative western blot of the NTS_2 receptor on cell lysate from MCF-7, MDA-MB-468, PC-3, SKBR3, T47-D, and ZR75.1 cells. (B) Semi-quantification of the NTS_2 signal from the western blots. (*) Data regarding NTS_2 expression on HT-29 cells are issued from our previous work.[24] Adapted with permission from Fanelli et al. *Bioconjugate Chemistry* 2020, 31, 10, 2339−2349. Copyright 2020 American Chemical Society.

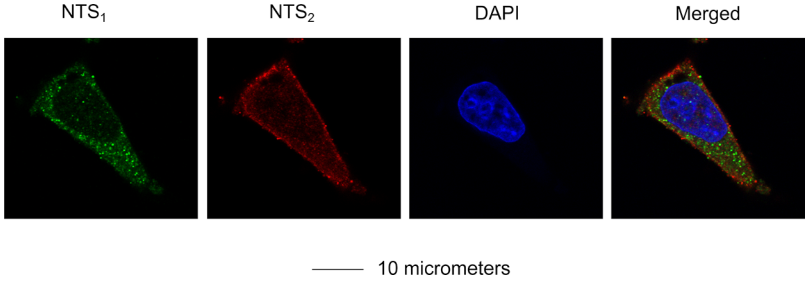

Figure 5. Confocal imaging of neurotensin receptors NTS_1 and NTS_2 on MCF-7 cells using indirect immunofluorescence. Images were obtained at 63× magnification. (NTS_1) intracytoplasmic granular expression of the NTS_1 receptor in MCF-7 cells. (NTS_2) Membrane expression of the NTS_2 receptor in MCF-7 cells. (DAPI) Nucleus staining of alive MCF-7cells using DAPI. (merged) Combination of NTS_1, NTS_2, and DAPI signal in MCF-7 cells.

corrected) and 63.75 ± 12.42% (^{111}In, decay corrected), high volumetric activities of 108.86 ± 15.24 (^{68}Ga) and 39.20 MBq/mL (^{111}In), and apparent molar activities of 8.77 ± 1.23 (^{68}Ga) and 2.95 GBq/μmol (^{111}In). Radiochemical purities were always >95%. No degradation of the radiolabeled product was observed in the vehicle over 8 days (on radio-HPLC analysis using the ^{111}In radiolabeled compound, Figure 2).

Human Blood Plasma Stability. Stability in human blood plasma was performed using [^{68}Ga]Ga-JMV 7488. At 15 min, 23.5% of the peptide remained intact and this value decreased up to 5% after 30 min (Figure 3).

***In Vitro* Studies.** NTS_2 expression has already been reported on HT-29 cells in previous studies.[24] To get further insight in the potential of NTS_2 in oncology, we performed western blot experiments on five breast cancer cell lines (MCF-7, MDA-MB-468, SKBR3, T47-D, and ZR75.1), on the prostate cancer cell line PC-3, and on the colorectal adenocarcinoma cell line HT-29. Semi-quantification of the

https://doi.org/10.1021/acsomega.2c07814
ACS Omega 2023, 8, 6994−7004

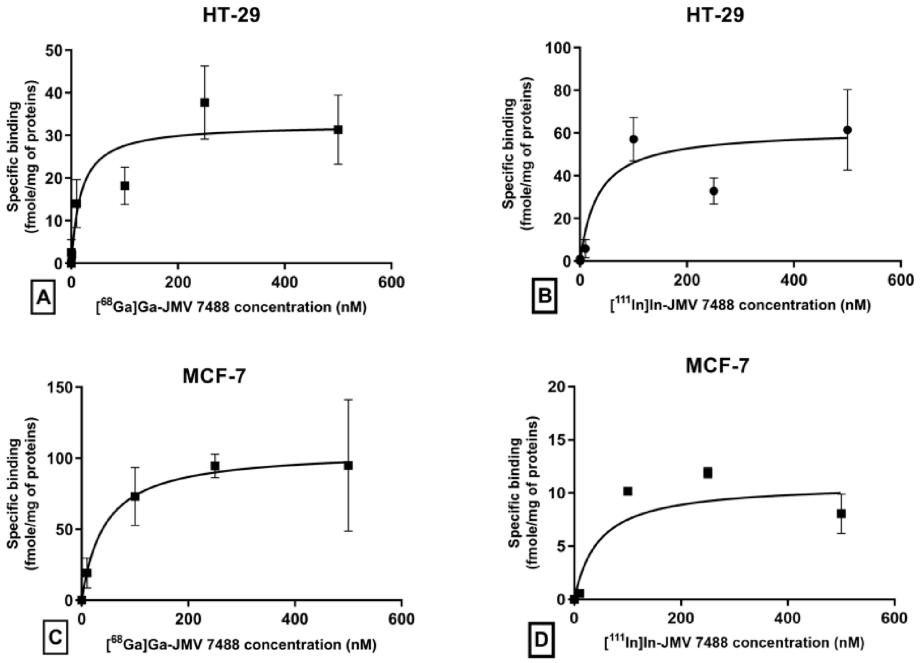

Figure 6. Saturation binding curves of [^{68}Ga]Ga-JMV 7488 on HT-29 cells (A) and MCF-7 cells (C) and [^{111}In]In-JMV 7488 on HT-29 cells (B) and MCF-7 cells (D) toward NTS_2. Blocking concentration of levocabastine = 1 μM.

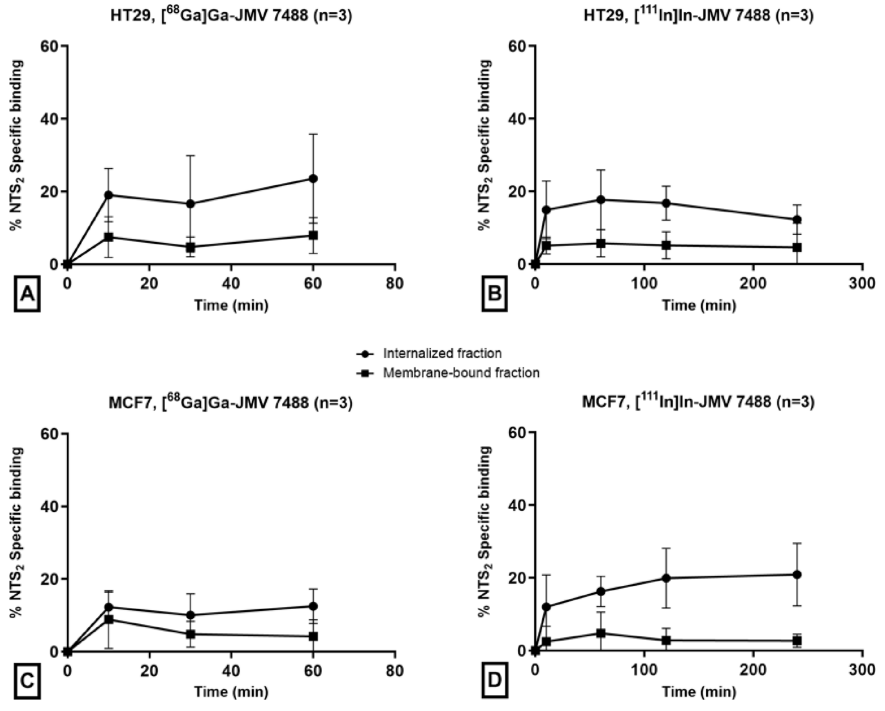

Figure 7. NTS_2 mediated internalizations of [^{68}Ga]Ga-JMV 7488 on HT-29 (A) and MCF-7(C) cells and [^{111}In]In-JMV 7488 on HT-29 (B) and MCF-7 (D) cells.

western blot showed that among the breast cancer cell line, the MCF-7 cells do express the highest level of NTS_2. HT-29 cells express the NTS_2 receptor. Lastly, PC-3 cells express the highest amount of NTS_2 among explored cancer cell lines (Figure 4).

Next, we performed confocal imaging on MCF-7 cells to assess the intracellular pattern of expression of NTS_2. As a validation step, we confirmed that MCF-7 cells express NTS_1 and that staining was intracytoplasmic and granular. Interestingly, MCF-7 cells express NTS_2 and the staining was mostly membranous as depicted in Figure 5. Negative controls did not exhibit staining.

Lipophilicity. $LogD_{7.4}$ values were -3.11 ± 0.24 for [^{68}Ga]Ga-JMV 7488 and -2.67 ± 0.18 for [^{111}In]-JMV 7488. Values were statistically significant ($p < 0.0001$).

Affinity Studies. Saturation binding studies performed on HT-29 and MCF-7 cells revealed that both [^{68}Ga]Ga-JMV 7488 and [^{111}In]In-JMV 7488 displayed a good affinity at

https://doi.org/10.1021/acsomega.2c07814
ACS Omega 2023, 8, 6994−7004

NTS_2 (Figure 6) and no specific binding at NTS_1 up to 0.5 μM. K_D values obtained were 37.83 ± 17.20 nM on HT-29 cells and 36.37 ± 9.89 nM on MCF-7 cells for [^{68}Ga]Ga-JMV 7488; 36.39 ± 4.02 nM on HT-29 cells and 45.94 ± 0.60 nM on MCF-7 cells for [^{111}In]In-JMV 7488. Bmax values at the NTS_2 receptor were 30.30 ± 18.46 fmol/mg of proteins on HT-29 cells and 50.15 ± 40.36 fmol/mg of proteins on MCF-7 cells (mean value obtained with [^{68}Ga]Ga-JMV 7488 and [^{111}In]In-JMV 7488).

Cell-Associated Radioactivity and Internalization Studies. After 1 h incubation at 37 °C, NTS_2-mediated uptakes (internalized and membranous) were 23.98 ± 4.79% of total binding for [^{68}Ga]Ga-JMV 7488 on HT-29 cells and 12.88 ± 8.23% on MCF-7, and for [^{111}In]In-JMV 7488, 19.72 ± 9.72 on HT-29 and 25.18 ± 11.73% on MCF-7 cells.

Kinetic studies (Figure 7) indicated that the internalized fraction rapidly reached its maximum 10 min after incubation and that this value remained stable over the experiment timeline (60 min for ^{68}Ga, 240 min for ^{111}In). The membrane-bound fraction was always below 8% of total binding.

Specific internalization represented 13.85 ± 9.75% of applied dose (AD) on HT-29 cells and 13.79 ± 4.78% AD on MCF-7 cells at 60 min.

Efflux Studies. [^{111}In]In-JMV 7488 demonstrated an intense efflux as early as 5 min (68.29 ± 19.30% on HT-29 cells and 54.34 ± 16.54% on MCF-7 cells). This value increased up to 78.06 ± 16.64% on HT-29 and 74.97 ± 9.56% on MCF-7 cells at 60 min and remained stable until 120 min (Figure 8). In prevision of *in vivo* experiments, efflux studies

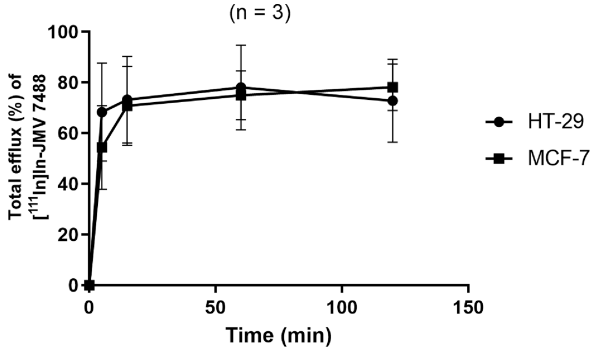

Figure 8. Total efflux of [^{111}In]In-JMV 7488 on HT-29 and MCF-7 cells.

were also performed with the gallium-68 radiolabeled compound on HT-29 cells. A similar behavior was seen with a high efflux rate of 45.28 ± 6.85% at 5 min, reaching 66.06 ± 8.05% at 45 min (data not shown).

Calcium Imaging Assay. Concentration-dependent Ca^{2+} mobilization was investigated with JMV 7488 and the NTS_2 agonist levocabastine as the positive control. EC_{50} values were 431 and 118 nM for JMV 7488 and levocabastine, respectively (Figure 9). JMV 7488 was able to promote the levocabastine-induced maximum dose−response (90.88 ± 11.49%), meaning that JMV 7488 is a full agonist at the NTS_2.

***In Vivo* Studies.** *Biodistribution Study.* Four mice were injected with 6.58 ± 1.54 MBq of [^{68}Ga]Ga-JMV 7488 and sacrificed 90 min after injection. Four other mice were co-injected with levocabastine (LV) along with 6.16 ± 1.21 MBq of [^{68}Ga]Ga-JMV 7488 to demonstrate the specificity of the binding. [^{68}Ga]Ga-JMV 7488 exhibited nonspecific uptake in

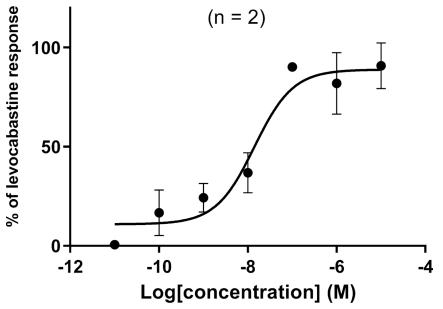

Figure 9. Intracellular mobilization of Ca^{2+} induced by JMV 7488. Results are normalized from stimulation induced by levocabastine.

kidneys (30.1 ± 18.4% ID/g) and prostate (2.25 ± 0.65% ID/g). Interestingly, HT-29 tumor and lungs showed specific uptake of [^{68}Ga]Ga-JMV 7488. The tumor/muscle ratio was significantly decreased when levocabastine was injected (5.5 ± 1.3 vs 1.7 ± 1.9 %ID/g, p = 0.02). Other organs did not show significant uptake (Figure 10 and Supporting Information Table S1).

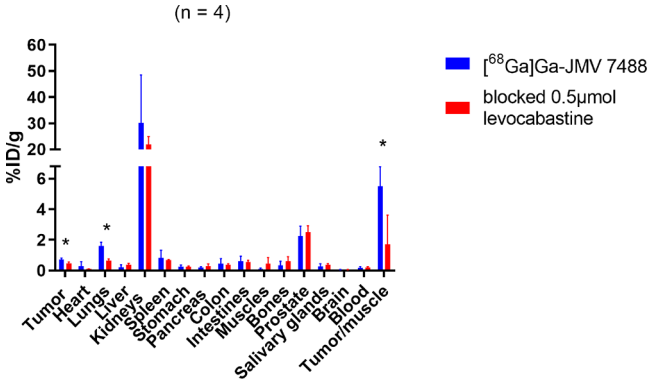

Figure 10. Biodistribution of [^{68}Ga]Ga-JMV 7488 injected in HT-29 xenografted mice. * indicates statistical differences (p < 0.05).

PET/CT Imaging. Whole-body μPET/CT imaging was performed on nude mice bearing HT-29 xenograft injected with [^{68}Ga]Ga-JMV 7488 without and with excess of levocabastine to assess NTS_2-specificity in vivo. Elimination of the radiotracer was urinary-exclusive. Unfortunately, no evident uptake on HT-29 was depicted on the PET/CT images at any time point (Figure 11).

DISCUSSION

Targeting neurotensin and its receptors holds promises in nuclear oncology.[25] The NTS_1 receptor has been shown to be over-expressed in several poor prognosis cancers such as pancreatic adenocarcinoma, triple negative breast cancer and glioblastoma among others.[26−28] However, little is known regarding the expression of the NTS_2 subtype in tumors and very few targeting biomolecules have been designed to target the NTS_2 subtype.[18] Thus, the aim of this work was to synthetize and characterize a new NTS_2-targeted radiolabeled peptide. As preliminary steps, NTS_2 expression was assessed in a panel of breast cancer cell lines and on a prostate cancer cell line using western blot. Results showed that expression of NTS_2 is variable across breast cancer cell lines, its over-expression being noticed in less aggressive phenotypes represented by MCF-7 and T47D cells (luminal A phenotype).

https://doi.org/10.1021/acsomega.2c07814
ACS Omega 2023, 8, 6994−7004

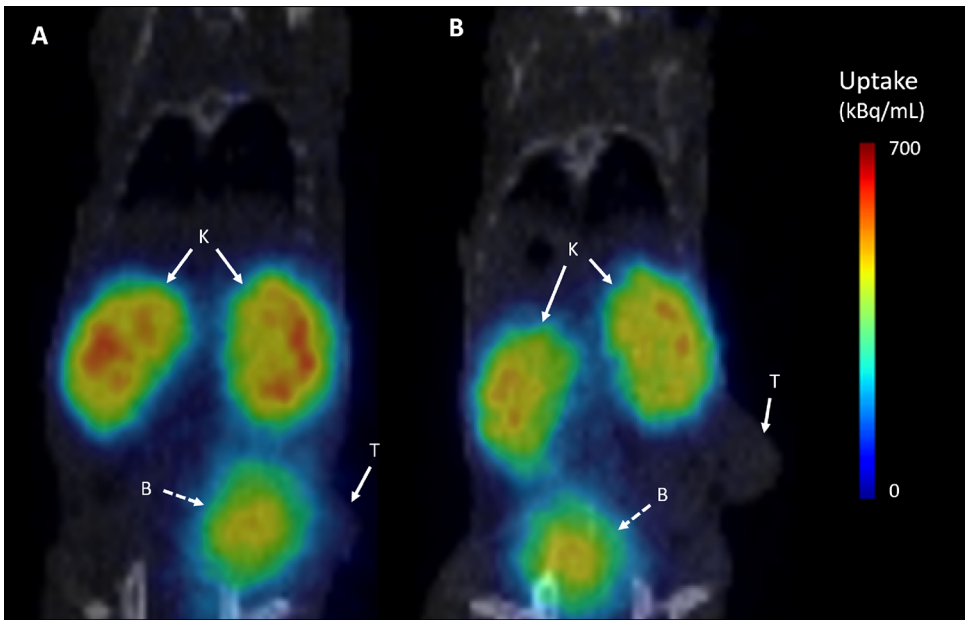

Figure 11. μPET/CT imaging of [^{68}Ga]Ga-JMV 7488 in HT-29 tumor-bearing nude mice. (A) Fused coronal PET/CT image at 75 min post-injection of a nude mice injected with 6 MBq of [^{68}Ga]Ga-JMV 7488 alone. (B) Fused coronal PET/CT image at 90 min post-injection of a nude mice co-injected with 6 MBq of [^{68}Ga]Ga-JMV 7488 and excess of levocabastine (0,5 μmole). K stands for kidneys, B is the bladder, and T is the HT-29 xenografted tumor.

Confocal imaging of NTS_1/NTS_2 expression was then assessed on the MCF-7 cell line, and the staining was membranous (Figure 4), which confirmed the rapid recycling properties of NTS_2 to the cell membrane upon stimulation.[29] In prostate cancer, the PC-3 cell line express an even higher amount of NTS_2. At last, we previously demonstrated that the colon cancer cell line HT-29 does express the NTS_2 subtype suggesting the potential of NTS_2 for imaging cancer types needing novel imaging strategies.[24] In this study, we were interested in developing a specific NTS_2-radiolabeled peptide (i.e., JMV 7488). HT-29 and MCF-7 cells were chose as models for preclinical characterization because (1) HT-29 is the standard cell line to characterize NTS_1-analogues, therefore allowing comparison, and (2) the MCF-7 cells, representing the luminal A breast cancer phenotype, need novel imaging agents to overpass intrinsic limitations of [^{18}F]-FDG.

Structurally, JMV 7488 is composed by a chelating agent (DOTA), two β-alanine (βAla) residues, and a modified NT sequence. While several chelating agents have been investigated,[30] DOTA is largely used for the development of radiopharmaceuticals.[31] The role of the linker between the chelating agents and the sequences responsible for the binding was widely discussed.[32,33] In JMV 7488, we inserted two βAla residues, with the aim to distance DOTA and the NT sequence. Regarding the latter, we and others identified the residue at the position 11 as being crucial for selectivity.[14,34−39] Considering the double interest of silicon-containing amino acids that confer both resistance to enzyme degradation and lipophilicity,[40] we also demonstrated that the replacement of Leu at position 13 by a TMSAla enhanced the binding affinity of NT ligands for both NTS_1 and NTS_2 by improving the interactions with the hydrophobic ligand binding pocket of both receptors.[41] More recently, we developed a series of modified NT analogues, in which some of them showed a NTS_1-mediated hypothermic effect.[22] Among all the analogues, the hexapeptide JMV 5504 (H-Lys-Lys-Pro-(D)Trp-Ile-TMSAla-OH) showed the best selectivity toward $hNTS_2$, with *Ki* values of 8.5 and 3600 nM toward $hNTS_2$ and $hNTS_1$, respectively (selectivity index $hNTS_1$/$hNTS_2$ = 423). Considering the poor NTS_1 binding affinity, no hypothermic effect for JMV 5504 was observed. In the light of our findings, the modified NT sequence of JMV 5504 was selected for the development of the first radiolabeled peptide targeting NTS_2 in peripheral tumors. The SPPS approach used for the synthesis of the desired product resulted to be really efficient, fast, and highly reproducible. After Fmoc-TMSAla-OH loading on 2-CTC resin, Fmoc-deprotections and couplings were carried out as we reported in detail in the Supporting Information. In this context, it has to be noted that the Kaiser test showed an uncomplete coupling reaction when Fmoc-Pro-OH, Fmoc-Lys-OH (for position 10), and DOTA(OtBu)$_3$-OH were used. For these reasons, the three above-mentioned coupling reactions were performed in duplicate. The final cleavage resulted to be very efficient after 7 h in vigorous shacking; meanwhile, shorter times have proved to be insufficient for a complete deprotection. In particular, by-products bearing -OtBu protecting groups were observed. After the cleavage, the desired NT analogue JMV 7488 was purified and characterized.

We first looked at the physicochemical parameters of [^{68}Ga]Ga-JMV 7488 and [^{111}In]In-JMV 7488 using the octanol/PBS partition coefficient method. We found that both radiotracers exhibit a marked hydrophilicity at pH 7.4, consistent with previous neurotensin analogues. Blood plasma stability of [^{68}Ga]Ga-JMV 7488 was tested on human plasma, and rapid cleavage was demonstrated (Figure 3). Strategies to improve the stability need to be carried out. They might include the use of enzyme inhibitors,[42] structural modification of the C-terminal hexapeptide binding sequence,[43] modification of the linker/chelate,[30] etc.

Radiolabeled JMV 7488 Were Then Investigated *In Vitro* on HT-29 Cells and MCF-7 Cells. Results from

https://doi.org/10.1021/acsomega.2c07814
ACS Omega 2023, 8, 6994−7004

saturation binding experiments showed that both radiolabeled bioconjugates exhibit a quite lower NTS_2 selectivity compared to the unconjugated counterpart JMV 5504.[22] Addition of the M^{3+}-DOTA-$(\beta Ala)_2$ moiety to the binding sequence results in the moderate loss of NTS_2 affinity (8.5 ± 2 nM [Ki] for JMV 5504 vs 38 ± 17 nM on HT-29 cells and 36 ± 10 nM on MCF-7 cells for [^{68}Ga]Ga-JMV 7488; 36 ± 4 nM on HT-29 cells and 46 ± 1 nM on MCF-7 cells for [^{111}In]In-JMV 7488). Interestingly, no NTS_1-binding was seen for both radiotracers indicating good selectivity (concentrations higher than 0.5 μM were not tested). The total number of NTS_2 receptor on HT-29 cells obtained by saturation binding experiment was consistent with previously published data.[44] We acknowledge that, compared to the ^{18}F-labeled NTS_2 glycopeptoid ^{18}F-**1**,[18] the NTS_2 affinities of our compounds were somewhat lower, but our radiolabeled peptides pave the way for the first time to NTS_2-directed imaging and treatment thanks to the DOTA macrocycle suitable for radiolabeling with radiometals for PET and/or TRT. This is not achievable with fluorine chemistry. Two other lessons can be deduced from these experiments. First, NTS_2 binding is not sensitive to hydrophilicity as [^{111}In]In-JMV 7488 was significantly less hydrophilic than [^{68}Ga]Ga-JMV 7488 without impact on NTS_2-binding. Second, HT-29 and MCF-7 cells provide same biological responses, indicating that breast cancer represents also an interesting model to study NTS_2-directed radiotracers. We encourage further studies in this setting.

Next, we investigated the intracellular behavior of [^{68}Ga]Ga-JMV 7488 in HT-29 cells and [^{111}In]In-JMV 7488 on MCF-7 cells. The high internalization rate of 20.53 ± 6.50% for [^{68}Ga]Ga-JMV 7488 is in line with its NTS_2 affinity. This value might appear low compared to the internalization capacity of NTS_1, which is about 70%, but one should keep in mind that the internalization process is the combination of several mechanisms including the β-arrestin coupling of the receptor and the recycling properties of the receptor. In the specific case of the NTS_2 receptor, β-arrestin coupling reached 85% of the specific binding similarly to NTS_1 but NTS_2 is rapidly recycled to the membrane contrarily to NTS_1, which is intracellularly retained.[29] Collectively, these data seem to indicate that our compounds promote high NTS_2-internalization, meaning that they behave like agonists regarding the NTS_2. The low membrane-bound fractions illustrate also well the supposed agonist behavior of [^{68}Ga]Ga-JMV 7488 and [^{111}In]In-JMV 7488 since agonists are internalized while antagonists usually do not. However, as the possibility for antagonists to undergo internalization has been highlighted,[45] we went deeper in its biological characterization by performing intracellular calcium mobilization experiments (Figure 9). As preliminary steps, we looked at the intracellular calcium mobilization of levocabastine as this point is still matter of debate[46] and was not explored in HT-29 cells. For the first time, we demonstrate that levocabastine is able to induce mobilization of intracellular calcium. Moreover, efficacy of JMV 7488 reaches the maximum intracellular calcium mobilization promoted by levocabastine, indicating that it is a full agonist at the NTS_2. The lower EC_{50} for JMV 7488 (411 vs 118 nM) reflects the lower NTS_2 affinity compared to levocabastine (this experiment was performed using the nonlabeled bioconjugate JMV 7488).

Efflux experiments were finally conducted, given the internalization of [^{68}Ga]Ga-JMV 7488 and [^{111}In]In-JMV 7488. Our results showed a high efflux, for both radiotracers (Figure 8). Overall, this is the first detailed *in vitro* characterization of a NTS_2-directed radiolabeled peptide for peripheral tumor imaging.

Because HT-29 tumors grow fast and do not require hormone supplementation and because of the possibility of quantification using PET, we choose to investigate [^{68}Ga]Ga-JMV 7488 *in vivo* in nude mice bearing HT-29 xenograft with the ^{68}Ga-labeled compound. Specificity of the binding was confirmed by displacement of 44% of [^{68}Ga]Ga-JMV 7488 signal by the NTS_2-preferring agonist levocabastine (full displacement was not reached). In biodistribution experiments performed 90 min after injection, uptake of [^{68}Ga]Ga-JMV 7488 in HT-29 tumor was still 0.72 ± 0.10%ID/g. Co-injection of levocabastine significantly decreased this value to 0.45 ± 0.10%ID/g, p = 0.03. In comparison with the ^{18}F-**1** agent developed by Prante's lab,[16] our compound provided a higher uptake in tumor at a later time point (90 min vs 60 min), which is a significant improvement. As expected, given the hydrophilicity of the radiotracer, [^{68}Ga]Ga-JMV 7488 was eliminated by the kidneys (Figure 11). Unfortunately, the uptake on HT-29 tumor was too low to build an image on the PET/CT presumably due to its low stability. The development of NTS_2-specific radiotracers allows a better knowledge of the distribution of NTS_2, and our study went deeper in this characterization compared to the literature. Our results provide for the first time evidence of an uptake [^{68}Ga]Ga-JMV 7488 in the mice prostate (translation to humans must be done carefully in the same way as the prostate specific membrane antigen (PSMA), which is expressed in mouse kidneys but absent in human kidneys). Although this nonspecific mechanism remains to be explored in details, this finding represents a caveat for the use of orthotopic models of primary prostate cancer to investigate NTS_2-targeting agents. Nevertheless, considering that in metastatic prostate cancer, tumor cells are disseminated outside the prostate bed, and that NTS_2 is expressed in PSMA-negative metastases (*i.e.*, PC-3 cells[18] and our data in this work), NTS_2-directed theranostic is appealing in case of [^{177}Lu]Lu-PSMA remains ineffective.[47] Moreover, NTS_2 is absent from salivary glands, which physiologically express the PSMA, therefore explaining xerostomia (partially) responsible for treatment discontinuation when using radiolabeled PSMA-inhibitors.[48] Moreover, the lungs showed moderate uptake of [^{68}Ga]Ga-JMV 7488 in line with the known expression of NTS_2.[21] Other organs do not retain significant uptake and therefore NTS_2 expression.

CONCLUSIONS

Collectively, targeting the NTS_2 subtype appears highly promising in phenotypes lacking imaging/therapeutic procedures such as low-FDG avid breast cancer cells, PSMA-negative prostate cancer cells, and colorectal cancer cells. Subsequent studies will further explore the expression profile of NTS_2 in human tumors and healthy tissues.

[^{68}Ga]Ga-JMV 7488 and [^{111}In]In-JMV 7488 showed good affinity and high internalization rate at the NTS_2. *In vivo*, [^{68}Ga]Ga-JMV 7488 showed moderate uptake on HT-29 tumors. Radiolabeled JMV 7488 behaves as a promising tool to assess NTS_2 expression in periphery. Further improvements in tumoral uptake and stability remain needed.

https://doi.org/10.1021/acsomega.2c07814
ACS Omega 2023, 8, 6994−7004

■ ASSOCIATED CONTENT

Supporting Information

The Supporting Information is available free of charge at https://pubs.acs.org/doi/10.1021/acsomega.2c07814.

Synthesis, analytical characterization of the desired NT analogue JMV 7488, radiolabeling procedures, determination of the octanol/water partition coefficient, cell culture, confocal imaging, *ex vivo* stability methods, and *ex vivo* biodistribution (PDF)

■ AUTHOR INFORMATION

Corresponding Authors

Florine Cavelier − *Institut des Biomolécules Max Mousseron, IBMM, UMR 5247, CNRS, Université de Montpellier, ENSCM, 34293 Montpellier, France;* orcid.org/0000-0001-5308-6416; Email: florine.cavelier@umontpellier.fr

Clément Morgat − *Department of Nuclear Medicine, University Hospital of Bordeaux, 33076 Bordeaux, France; University of Bordeaux, CNRS, EPHE, INCIA, UMR 5287, Bordeaux F-33000, France;* orcid.org/0000-0002-9432-9223; Email: clement.morgat@u-bordeaux.fr, clement.morgat@chu-bordeaux.fr

Authors

Sacha Bodin − *Department of Nuclear Medicine, University Hospital of Bordeaux, 33076 Bordeaux, France; University of Bordeaux, CNRS, EPHE, INCIA, UMR 5287, Bordeaux F-33000, France;* orcid.org/0000-0001-7331-8536

Santo Previti − *Institut des Biomolécules Max Mousseron, IBMM, UMR 5247, CNRS, Université de Montpellier, ENSCM, 34293 Montpellier, France*

Emmanuelle Jestin − *Cyclotron Réunion Océan Indien CYROI, 97490 Sainte Clotilde, France*

Delphine Vimont − *University of Bordeaux, CNRS, EPHE, INCIA, UMR 5287, Bordeaux F-33000, France*

Imade Ait-Arsa − *Cyclotron Réunion Océan Indien CYROI, 97490 Sainte Clotilde, France*

Frédéric Lamare − *Department of Nuclear Medicine, University Hospital of Bordeaux, 33076 Bordeaux, France; University of Bordeaux, CNRS, EPHE, INCIA, UMR 5287, Bordeaux F-33000, France*

Emmanuelle Rémond − *Institut des Biomolécules Max Mousseron, IBMM, UMR 5247, CNRS, Université de Montpellier, ENSCM, 34293 Montpellier, France;* orcid.org/0000-0002-3201-4365

Elif Hindié − *Department of Nuclear Medicine, University Hospital of Bordeaux, 33076 Bordeaux, France; University of Bordeaux, CNRS, EPHE, INCIA, UMR 5287, Bordeaux F-33000, France; Institut Universitaire de France, 75231 Paris, France*

Complete contact information is available at: https://pubs.acs.org/10.1021/acsomega.2c07814

Author Contributions

#F.C. and C.M. contributed equally to directing this study. S.P. and E.R. synthetized and purified the JMV 7488 compound. S.B., D.V., and C.M. performed radiolabeling and in vitro experiments and analyzed data. I.A.A. and E.J. performed in vivo experiments. F.L. analyzed microPET data. E.H. critically reviewed the manuscript. The manuscript was written through contributions of all authors. All authors have given approval to the final version of the manuscript.

Funding

This work was partly funded by the Institut National du Cancer (INCa PLBIO 2017, THERACAN project) and by France Life Imaging (FLI). This study was conducted in the framework of the University of Bordeaux IdEx "Investments for the Future" program RRI "NewMOON" that received financial support from the French Government.

Notes

The authors declare no competing financial interest.

■ ACKNOWLEDGMENTS

INCa is acknowledged for postdoctoral fellowship to S.P. The calcium imaging experiments were done at the Phycell facility, Institut de Neurosciences Cognitives et Integratives d'Aquitaine.

■ ABBREVIATIONS

^{68}Ga, gallium 68; ^{111}In, indium-111; FBS, fetal bovine serum; GPCR, G protein-coupled receptors; HPLC, high-performance liquid chromatography; PBS, phosphate buffered saline; NT, neurotensin; NTS_1, NT receptor 1; NTS_2, NT receptor 2; TFA, trifluoroacetic acid; TLC, thin layer chromatography; TMSAla, (L)-(trimethylsilyl)alanine.

■ REFERENCES

(1) Davenport, A. P.; Scully, C. C. G.; de Graaf, C.; Brown, A. J. H.; Maguire, J. J. Advances in Therapeutic Peptides Targeting G Protein-Coupled Receptors. *Nat Rev Drug Discov* **2020**, *19*, 389−413.

(2) Carraway, R.; Leeman, S. E. The Isolation of a New Hypotensive Peptide, Neurotensin, from Bovine Hypothalami. *J. Biol. Chem.* **1973**, *248*, 6854−6861.

(3) St-Gelais, F.; Jomphe, C.; Trudeau, L.-E. The Role of Neurotensin in Central Nervous System Pathophysiology: What Is the Evidence? *J. Psychiatry Neurosci.* **2006**, *31*, 229−245.

(4) Vita, N.; Laurent, P.; Lefort, S.; Chalon, P.; Dumont, X.; Kaghad, M.; Gully, D.; Le Fur, G.; Ferrara, P.; Caput, D. Cloning and Expression of a Complementary DNA Encoding a High Affinity Human Neurotensin Receptor. *FEBS Lett.* **1993**, *317*, 139.

(5) Schulz, S.; Röcken, C.; Ebert, M. P. A.; Schulz, S. Immunocytochemical Identification of Low-Affinity NTS_2 Neurotensin Receptors in Parietal Cells of Human Gastric Mucosa. *J Endocrinol* **2006**, *191*, 121−128.

(6) Barroso, S.; Richard, F.; Nicolas-Ethève, D.; Reversat, J.-L.; Bernassau, J.-M.; Kitabgi, P.; Labbé-Jullié, C. Identification of Residues Involved in Neurotensin Binding and Modeling of the Agonist Binding Site in Neurotensin Receptor 1. *J. Biol. Chem.* **2000**, *275*, 328−336.

(7) Gonzalez, S.; Dumitrascuta, M.; Eiselt, E.; Louis, S.; Kunze, L.; Blasiol, A.; Vivancos, M.; Previti, S.; Dewolf, E.; Martin, C.; Tourwé, D.; Cavelier, F.; Gendron, L.; Sarret, P.; Spetea, M.; Ballet, S. Optimized Opioid-Neurotensin Multitarget Peptides: From Design to Structure−Activity Relationship Studies. *J. Med. Chem.* **2020**, *63*, 12929−12941.

(8) Buchegger, F.; Bonvin, F.; Kosinski, M.; Schaffland, A. O.; Prior, J.; Reubi, J. C.; Bläuenstein, P.; Tourwé, D.; Garayoa, E. G.; Delaloye, A. B. Radiolabeled Neurotensin Analog, ^{99m}Tc-NT-XI, Evaluated in Ductal Pancreatic Adenocarcinoma Patients. *J. Nucl. Med.* **2003**, *44*, 1649−1654.

(9) Maschauer, S.; Einsiedel, J.; Hübner, H.; Gmeiner, P.; Prante, O. ^{18}F- and ^{68}Ga-Labeled Neurotensin Peptides for PET Imaging of Neurotensin Receptor 1. *J. Med. Chem.* **2016**, *59*, 6480−6492.

(10) Prignon, A.; Provost, C.; Alshoukr, F.; Wendum, D.; Couvelard, A.; Barbet, J.; Forgez, P.; Talbot, J.-N.; Gruaz-Guyon, A. Preclinical Evaluation of ^{68}Ga-DOTA-NT-20.3: A Promising PET Imaging Probe To Discriminate Human Pancreatic Ductal Adenocarcinoma from Pancreatitis. *Mol. Pharmaceutics* **2019**, *16*, 2776−2784.

(11) Alshoukr, F.; Prignon, A.; Brans, L.; Jallane, A.; Mendes, S.; Talbot, J.-N.; Tourwé, D.; Barbet, J.; Gruaz-Guyon, A. Novel DOTA-Neurotensin Analogues for ^{111}In Scintigraphy and ^{68}Ga PET Imaging of Neurotensin Receptor-Positive Tumors. *Bioconjugate Chem.* **2011**, *22*, 1374−1385.
(12) Deng, H.; Wang, H.; Zhang, H.; Wang, M.; Giglio, B.; Ma, X.; Jiang, G.; Yuan, H.; Wu, Z.; Li, Z. Imaging Neurotensin Receptor in Prostate Cancer With ^{64}Cu-Labeled Neurotensin Analogs. *Mol Imaging* **2017**, *16*, 1536012117711369.
(13) Held, C.; Plomer, M.; Hübner, H.; Meltretter, J.; Pischetsrieder, M.; Gmeiner, P. Development of a Metabolically Stable Neurotensin Receptor 2 (NTS_2) Ligand. *ChemMedChem* **2013**, *8*, 75−81.
(14) Eiselt, E.; Gonzalez, S.; Martin, C.; Chartier, M.; Betti, C.; Longpré, J.-M.; Cavelier, F.; Tourwé, D.; Gendron, L.; Ballet, S.; Sarret, P. Neurotensin Analogues Containing Cyclic Surrogates of Tyrosine at Position 11 Improve NTS_2 Selectivity Leading to Analgesia without Hypotension and Hypothermia. *ACS Chem. Neurosci.* **2019**, *10*, 4535−4544.
(15) Besserer-Offroy, É.; Brouillette, R. L.; Lavenus, S.; Froehlich, U.; Brumwell, A.; Murza, A.; Longpré, J.-M.; Marsault, É.; Grandbois, M.; Sarret, P.; Leduc, R. The Signaling Signature of the Neurotensin Type 1 Receptor with Endogenous Ligands. *Eur. J. Pharmacol.* **2017**, *805*, 1−13.
(16) Tétreault, P.; Besserer-Offroy, É.; Brouillette, R. L.; René, A.; Murza, A.; Fanelli, R.; Kirby, K.; Parent, A. J.; Dubuc, I.; Beaudet, N.; Côté, J.; Longpré, J.-M.; Martinez, J.; Cavelier, F.; Sarret, P. Pain Relief Devoid of Opioid Side Effects Following Central Action of a Silylated Neurotensin Analog. *Eur. J. Pharmacol.* **2020**, *882*, 173174.
(17) Vivancos, M.; Fanelli, R.; Besserer-Offroy, É.; Beaulieu, S.; Chartier, M.; Resua-Rojas, M.; Mona, C. E.; Previti, S.; Rémond, E.; Longpré, J.-M.; Cavelier, F.; Sarret, P. Metabolically Stable Neurotensin Analogs Exert Potent and Long-Acting Analgesia without Hypothermia. *Behav Brain Res* **2021**, *405*, 113189.
(18) Maschauer, S.; Greff, C.; Einsiedel, J.; Ott, J.; Tripal, P.; Hübner, H.; Gmeiner, P.; Prante, O. Improved Radiosynthesis and Preliminary in Vivo Evaluation of a ^{18}F-Labeled Glycopeptide−Peptoid Hybrid for PET Imaging of Neurotensin Receptor 2. *Bioorg. Med. Chem.* **2015**, *23*, 4026−4033.
(19) Swift, S. L.; Burns, J. E.; Maitland, N. J. Altered Expression of Neurotensin Receptors Is Associated with the Differentiation State of Prostate Cancer. *Cancer Res.* **2010**, *70*, 347−356.
(20) Abbaci, A.; Talbot, H.; Saada, S.; Gachard, N.; Abraham, J.; Jaccard, A.; Bordessoule, D.; Fauchais, A. L.; Naves, T.; Jauberteau, M. O. Neurotensin Receptor Type 2 Protects B-Cell Chronic Lymphocytic Leukemia Cells from Apoptosis. *Oncogene* **2018**, *37*, 756−767.
(21) Vita, N.; Oury-Donat, F.; Chalon, P.; Guillemot, M.; Kaghad, M.; Bachy, A.; Thurneyssen, O.; Garcia, S.; Poinot-Chazel, C.; Casellas, P.; Keane, P.; Le Fur, G.; Maffrand, J. P.; Soubrie, P.; Caput, D.; Ferrara, P. Neurotensin Is an Antagonist of the Human Neurotensin NT2 Receptor Expressed in Chinese Hamster Ovary Cells. *Eur. J. Pharmacol.* **1998**, *360*, 265−272.
(22) Previti, S.; Vivancos, M.; Rémond, E.; Beaulieu, S.; Longpré, J.-M.; Ballet, S.; Sarret, P.; Cavelier, F. Insightful Backbone Modifications Preventing Proteolytic Degradation of Neurotensin Analogs Improve NTS_1-Induced Protective Hypothermia. *Front. Chem.* **2020**, *8*, 406.
(23) René, A.; Vanthuyne, N.; Martinez, J.; Cavelier, F. (L)-(Trimethylsilyl)Alanine Synthesis Exploiting Hydroxypinanone-Induced Diastereoselective Alkylation. *Amino Acids* **2013**, *45*, 301−307.
(24) Fanelli, R.; Chastel, A.; Previti, S.; Hindié, E.; Vimont, D.; Zanotti-Fregonara, P.; Fernandez, P.; Garrigue, P.; Lamare, F.; Schollhammer, R.; Balasse, L.; Guillet, B.; Rémond, E.; Morgat, C.; Cavelier, F. Silicon-Containing Neurotensin Analogues as Radiopharmaceuticals for NTS_1-Positive Tumors Imaging. *Bioconjugate Chem.* **2020**, *31*, 2339−2349.
(25) Morgat, C.; Mishra, A. K.; Varshney, R.; Allard, M.; Fernandez, P.; Hindié, E. Targeting Neuropeptide Receptors for Cancer Imaging and Therapy: Perspectives with Bombesin, Neurotensin, and Neuropeptide-Y Receptors. *J. Nucl. Med.* **2014**, *55*, 1650−1657.
(26) Morgat, C.; Brouste, V.; Chastel, A.; Vélasco, V.; Macgrogan, G.; Hindié, E. Expression of Neurotensin Receptor-1 (NTS1) in Primary Breast Tumors, Cellular Distribution, and Association with Clinical and Biological Factors. *Breast Cancer Res. Treat.* **2021**, *190*, 403−413.
(27) Körner, M.; Waser, B.; Strobel, O.; Büchler, M.; Reubi, J. C. Neurotensin Receptors in Pancreatic Ductal Carcinomas. *EJNMMI Res.* **2015**, *5*, DOI: 10.1186/s13550-015-0094-2.
(28) Ouyang, Q.; Chen, G.; Zhou, J.; Li, L.; Dong, Z.; Yang, R.; Xu, L.; Cui, H.; Xu, M.; Yi, L. Neurotensin Signaling Stimulates Glioblastoma Cell Proliferation by Upregulating C-Myc and Inhibiting MiR-29b-1 and MiR-129-3p. *Neuro Oncol* **2016**, *18*, 216−226.
(29) Martin, S.; Vincent, J.-P.; Mazella, J. Recycling Ability of the Mouse and the Human Neurotensin Type 2 Receptors Depends on a Single Tyrosine Residue. *J. Cell Sci.* **2002**, *115*, 165−173.
(30) Renard, E.; Moreau, M.; Bellaye, P.-S.; Guillemin, M.; Collin, B.; Prignon, A.; Denat, F.; Goncalves, V. Positron Emission Tomography Imaging of Neurotensin Receptor-Positive Tumors with ^{68}Ga-Labeled Antagonists: The Chelate Makes the Difference Again. *J. Med. Chem.* **2021**, *64*, 8564−8578.
(31) Baranyai, Z.; Tircsó, G.; Rösch, F. The Use of the Macrocyclic Chelator DOTA in Radiochemical Separations. *Eur. J. Inorg. Chem.* **2020**, *2020*, 36−56.
(32) Kim, Y.-S.; Yang, C.-T.; Wang, J.; Wang, L.; Li, Z.-B.; Chen, X.; Liu, S. Effects of Targeting Moiety, Linker, Bifunctional Chelator, and Molecular Charge on Biological Properties of ^{64}Cu-Labeled Triphenylphosphonium Cations. *J. Med. Chem.* **2008**, *51*, 2971−2984.
(33) Tolmachev, V.; Feldwisch, J.; Lindborg, M.; Baastrup, B.; Sandström, M.; Orlova, A. Influence of an Aliphatic Linker between DOTA and Synthetic Z(HER2:342) Affibody Molecule on Targeting Properties of the ^{111}In-Labeled Conjugate. *Nucl. Med. Biol.* **2011**, *38*, 697−706.
(34) Hapău, D.; Rémond, E.; Fanelli, R.; Vivancos, M.; René, A.; Côté, J.; Besserer-Offroy, É.; Longpré, J.-M.; Martinez, J.; Zaharia, V.; Sarret, P.; Cavelier, F. Stereoselective Synthesis of β-(5-Arylthiazolyl) α-Amino Acids and Use in Neurotensin Analogues. *Eur. J. Org. Chem.* **2016**, *2016*, 1017−1024.
(35) Einsiedel, J.; Held, C.; Hervet, M.; Plomer, M.; Tschammer, N.; Hübner, H.; Gmeiner, P. Discovery of Highly Potent and Neurotensin Receptor 2 Selective Neurotensin Mimetics. *J. Med. Chem.* **2011**, *54*, 2915−2923.
(36) Boules, M.; Johnston, H.; Tozy, J.; Smith, K.; Li, Z.; Richelson, E. Analgesic Synergy of Neurotensin Receptor Subtype 2 Agonist NT79 and Morphine. *Behav. Pharmacol.* **2011**, *22*, 573−581.
(37) Boules, M.; Shaw, A.; Liang, Y.; Barbut, D.; Richelson, E. NT69L, a Novel Analgesic, Shows Synergy with Morphine. *Brain Res.* **2009**, *1294*, 22−28.
(38) Fanelli, R.; Floquet, N.; Besserer-Offroy, É.; Delort, B.; Vivancos, M.; Longpré, J.-M.; Renault, P.; Martinez, J.; Sarret, P.; Cavelier, F. Use of Molecular Modeling to Design Selective NTS_2 Neurotensin Analogues. *J. Med. Chem.* **2017**, *60*, 3303−3313.
(39) Previti, S.; Desgagné, M.; Tourwé, D.; Cavelier, F.; Sarret, P.; Ballet, S. Opening the Amino Acid Toolbox for Peptide-Based NTS_2-Selective Ligands as Promising Lead Compounds for Pain Management. *J. Pept. Sci.* , e3471, DOI: 10.1002/psc.3471.
(40) Rémond, E.; Martin, C.; Martinez, J.; Cavelier, F. Silicon-Containing Amino Acids: Synthetic Aspects, Conformational Studies, and Applications to Bioactive Peptides. *Chem. Rev.* **2016**, *116*, 11654−11684.
(41) Fanelli, R.; Besserer-Offroy, É.; René, A.; Côté, J.; Tétreault, P.; Collerette-Tremblay, J.; Longpré, J.-M.; Leduc, R.; Martinez, J.; Sarret, P.; Cavelier, F. Synthesis and Characterization in Vitro and in Vivo of (L)-(Trimethylsilyl)Alanine Containing Neurotensin Analogues. *J. Med. Chem.* **2015**, *58*, 7785−7795.
(42) Kanellopoulos, P.; Nock, B. A.; Krenning, E. P.; Maina, T. Optimizing the Profile of [^{99m}Tc]Tc-NT(7-13) Tracers in Pancreatic

https://doi.org/10.1021/acsomega.2c07814
ACS Omega 2023, 8, 6994−7004

Cancer Models by Means of Protease Inhibitors. *Int. J. Mol. Sci.* **2020**, *21*, 7926.
(43) Magafa, V.; Matsoukas, M.-T.; Karageorgos, V.; Dermitzaki, E.; Exarchakou, R.; Stylos, E. K.; Pardalos, M.; Margioris, A. N.; Varvounis, G.; Tzakos, A. G.; Spyroulias, G. A.; Liapakis, G. Novel Stable Analogues of the Neurotensin C-Terminal Hexapeptide Containing Unnatural Amino Acids. *Amino Acids* **2019**, *51*, 1009−1022.
(44) Maoret, J. J.; Pospaï, D.; Rouyer-Fessard, C.; Couvineau, A.; Laboisse, C.; Voisin, T.; Laburthe, M. Neurotensin Receptor and Its MRNA Are Expressed in Many Human Colon Cancer Cell Lines but Not in Normal Colonic Epithelium: Binding Studies and RT-PCR Experiments. *Biochem. Biophys. Res. Commun.* **1994**, *203*, 465−471.
(45) Pheng, L. H.; Dumont, Y.; Fournier, A.; Chabot, J.-G.; Beaudet, A.; Quirion, R. Agonist- and Antagonist-Induced Sequestration/Internalization of Neuropeptide Y Y_1 Receptors in HEK293 Cells. *Br. J. Pharmacol.* **2003**, *139*, 695−704.
(46) Mazella, J.; Vincent, J.-P. Internalization and Recycling Properties of Neurotensin Receptors. *Peptides* **2006**, *27*, 2488−2492.
(47) Hofman, M. S.; Emmett, L.; Sandhu, S.; Iravani, A.; Joshua, A. M.; Goh, J. C.; Pattison, D. A.; Tan, T. H.; Kirkwood, I. D.; Ng, S.; Francis, R. J.; Gedye, C.; Rutherford, N. K.; Weickhardt, A.; Scott, A. M.; Lee, S.-T.; Kwan, E. M.; Azad, A. A.; Ramdave, S.; Redfern, A. D.; Macdonald, W.; Guminski, A.; Hsiao, E.; Chua, W.; Lin, P.; Zhang, A. Y.; McJannett, M. M.; Stockler, M. R.; Violet, J. A.; Williams, S. G.; Martin, A. J.; Davis, I. D.; TheraP Trial Investigators and the Australian and New Zealand Urogenital and Prostate Cancer Trials Group. TheraP Trial Investigators and the Australian and New Zealand Urogenital and Prostate Cancer Trials Group. [^{177}Lu]Lu-PSMA-617 versus Cabazitaxel in Patients with Metastatic Castration-Resistant Prostate Cancer (TheraP): A Randomised, Open-Label, Phase 2 Trial. *Lancet* **2021**, *397*, 797−804.
(48) Feuerecker, B.; Tauber, R.; Knorr, K.; Heck, M.; Beheshti, A.; Seidl, C.; Bruchertseifer, F.; Pickhard, A.; Gafita, A.; Kratochwil, C.; Retz, M.; Gschwend, J. E.; Weber, W. A.; D'Alessandria, C.; Morgenstern, A.; Eiber, M. Activity and Adverse Events of Actinium-225-PSMA-617 in Advanced Metastatic Castration-Resistant Prostate Cancer After Failure of Lutetium-177-PSMA. *Eur. Urol.* **2021**, *79*, 343−350.

https://doi.org/10.1021/acsomega.2c07814
ACS Omega 2023, 8, 6994−7004